Neutrophils recruited by chemoattractants in vivo induce microvascular plasma protein leakage through secretion of TNF

Michaela Finsterbusch,[1] Mathieu-Benoit Voisin,[1] Martina Beyrau,[1] Timothy John Williams,[1,2] and Sussan Nourshargh[1]

[1]William Harvey Research Institute, Barts and the London School of Medicine and Dentistry, Queen Mary University of London, London E1 4NS, England, UK
[2]National Heart and Lung Institute, Faculty of Medicine, Imperial College London, London SW7 2AZ, England, UK

Microvascular plasma protein leakage is an essential component of the inflammatory response and serves an important function in local host defense and tissue repair. Mediators such as histamine and bradykinin act directly on venules to increase the permeability of endothelial cell (EC) junctions. Neutrophil chemoattractants also induce leakage, a response that is dependent on neutrophil adhesion to ECs, but the underlying mechanism has proved elusive. Through application of confocal intravital microscopy to the mouse cremaster muscle, we show that neutrophils responding to chemoattractants release TNF when in close proximity of EC junctions. In vitro, neutrophils adherent to ICAM-1 or ICAM-2 rapidly released TNF in response to LTB_4, C5a, and KC. Further, in $TNFR^{-/-}$ mice, neutrophils accumulated normally in response to chemoattractants administered to the cremaster muscle or dorsal skin, but neutrophil-dependent plasma protein leakage was abolished. Similar results were obtained in chimeric mice deficient in leukocyte TNF. A locally injected TNF blocking antibody was also able to inhibit neutrophil-dependent plasma leakage, but had no effect on the response induced by bradykinin. The results suggest that TNF mediates neutrophil-dependent microvascular leakage. This mechanism may contribute to the effects of TNF inhibitors in inflammatory diseases and indicates possible applications in life-threatening acute edema.

In response to an inflammatory stimulus, priorities change with respect to the maintenance of tissue homeostasis. Under basal conditions, the microvascular endothelium has a low permeability to plasma proteins and forms a barrier between high intravascular and low extravascular interstitial fluid protein concentrations. This provides an oncotic gradient that balances the opposing hydrostatic pressure gradient that would otherwise move water and small solutes from the blood to the tissues, with any small net outflow being compensated by lymphatic drainage. After the detection of potentially harmful substances, foreign organisms, or injured tissue cells, the immediate priority is to supply plasma proteins to the extravascular compartment. This delivers immunoglobulins, constituents of the complement and coagulation systems, antiproteases, and other acute phase reactants to the

site to participate in local host defense and the initiation of tissue repair. The compromise to homeostasis results in tissue edema (an example of *functio laesa*). Tissue mast cells act as sentinel cells and provide one means of detecting potentially harmful agents by means of an array of receptors, including Toll-like receptors and IgE bound to FcεR1. Mast cells release histamine that induces plasma leakage by acting directly on histamine receptors located on the venular endothelium, the region of the microvasculature specialized for permeability responses (Majno and Palade, 1961). Increased permeability is dependent on a destabilization of the VE-cadherin–catenin complex and its interaction with the actin cytoskeleton at EC junctions (Yuan, 2002; Schulte et al., 2011). Other

M.-B. Voisin and M. Beyrau contributed equally to this paper.

The Rockefeller University Press $30.00
J. Exp. Med. 2014 Vol. 211 No. 7   1307-1314
www.jem.org/cgi/doi/10.1084/jem.20132413

1307

The Journal of Experimental Medicine

such mediators acting directly on ECs include bradykinin, peptidoleukotrienes, platelet-activating factor, and VEGF.

Inflammatory stimuli also trigger the local production of chemoattractants that induce acute neutrophil infiltration. Once accumulated and interacting with the potentially injurious stimulus, these cells were generally accepted to contribute to tissue swelling in the later stages of inflammation by releasing substances that damage the endothelium, such as proteases and reactive oxygen species. Subsequent observations suggested another link between neutrophils and increased microvascular permeability by a mechanism that could operate in the very early stages of the inflammatory response. The neutrophil chemoattractants C5a, leukotriene B_4 (LTB$_4$), and fMLP were found to induce significantly increased EC permeability within 6 min of injection into animal skin, and these responses were absent in animals depleted of their circulating neutrophils (Wedmore and Williams, 1981). This led to the conclusion that neutrophils responding to a chemoattractant signal can rapidly increase the permeability of EC junctions when the leukocytes are in close apposition to venular ECs; thus, regulating the supply of plasma proteins to the extravascular space. This concept was supported by studies in which a blocking anti-β_2 integrin mAb was found to inhibit neutrophil-dependent edema (Arfors et al., 1987). Collectively, neutrophil chemoattractants, including chemokines, have been found to increase microvascular permeability in several animal species (Wedmore and Williams, 1981; Williams and Jose, 1981; Björk et al., 1982; Tokita and Yamamoto, 2004), and responses to intradermal C5a have been shown to be markedly reduced in neutropenic human subjects (Williamson et al., 1986; Yancey et al., 1987).

The perivascular basement membrane (BM) is permeable to plasma proteins and allows their entry into tissues when EC junctions open. Large colloidal molecules administered into the systemic circulation are, however, trapped under the BM/pericyte layer, which is the basis of the vascular labeling technique that first identified venules as the site of action of histamine (Majno and Palade, 1961). Some early studies showed that neutrophils can disrupt the perivascular BM so that large colloidal molecules can pass through (Hurley, 1964; Huber and Weiss, 1989). These observations may relate to our previous findings that show changes in BM morphology and enlarged gaps between pericytes induced by inflammatory mediators in vivo (Wang et al., 2006; Voisin et al., 2009; Proebstl et al., 2012). In extending these findings, we noted that neutrophil chemoattractants induced pericyte shape change in vivo in a neutrophil-dependent manner, and that this response was mediated by endogenously generated TNF. Because, in response to chemoattractants, neutrophils within the vascular lumen expressed TNF in close proximity of EC junctions and TNF increases microvascular permeability to plasma proteins (Brett et al., 1989), we investigated if neutrophil-derived TNF could also provide an important link between neutrophils and increased endothelial permeability. The present results provide direct evidence for the ability of endogenous neutrophil-derived TNF to mediate chemoattractant-induced increased microvascular permeability and describe a potential mechanism for neutrophil-dependent edema.

RESULTS AND DISCUSSION

Neutrophil chemoattractants induce generation of TNF in vivo

As part of our investigations into the impact of proinflammatory mediators on venular morphology in vivo (Voisin et al., 2010; Proebstl et al., 2012), we noted that locally administered neutrophil chemoattractants can induce pericyte shape change in mouse cremaster postcapillary venules in a TNF-dependent manner (Fig. 1, A and B). Specifically, intrascrotal administration of the chemoattractants LTB$_4$, C5a, and KC (CXCL1) caused pericyte shape change in WT mice, as indicated by an increase in gaps between adjacent pericytes. These effects were totally absent in TNFR$^{-/-}$ mice (Fig. 1 B), suggesting that chemoattractants can induce the generation of endogenous TNF in close proximity to venular walls. As expected, the response to exogenous TNF was also abolished in the TNFR$^{-/-}$ mice (Fig. 1 B). LTB$_4$, C5a, and KC did not induce pericyte shape change in neutrophil-depleted mice (Fig. 1 C), indicating that the generated TNF was derived from neutrophils.

TNF is associated with neutrophils adherent to venular ECs in LTB$_4$–stimulated tissues in vivo

To gain a better understanding of the functional role of endogenously generated TNF, we sought to investigate the site and dynamics of TNF release in response to neutrophil chemotactic mediators in vivo. Initial in vitro studies provided direct evidence for the existence of preformed intracellular TNF stores in mouse blood neutrophils and the ability of these cells to rapidly release TNF in response to LTB$_4$ (Fig. 2, A and D). This was shown by the time-dependent loss of intracellular TNF in neutrophils stimulated with LTB$_4$ (Fig. 2, A, B, and D) and by the detection of soluble TNF in supernatants of these cells (Fig. 2 C). To investigate the dynamics of TNF release from neutrophils within microvessels of chemoattractant-stimulated tissues in vivo, a protocol was developed for detecting expression of TNF during early neutrophil–venular wall interactions. Cremaster muscles of *Lys-EGFP-ki* mice were examined by confocal intravital microscopy as previously detailed (Woodfin et al., 2011). Furthermore, in vivo immunostaining of EC junctions using an anti–PECAM-1 mAb allowed tracking of GFP^{high} neutrophil responses within the venular lumen, neutrophil transendothelial cell migration (TEM), and neutrophil sub–EC migration (Woodfin et al., 2011; Proebstl et al., 2012). This previously established protocol was extended to enable us to simultaneously visualize the localization of TNF as detected by an i.v. injected fluorescently labeled anti–TNF mAb. Using this approach, no TNF was detected during the early steps of neutrophil adhesion and crawling along the luminal side of ECs after topical LTB$_4$ application (Fig. 2, E and F). However, TNF could be detected on the surface of neutrophils a few minutes
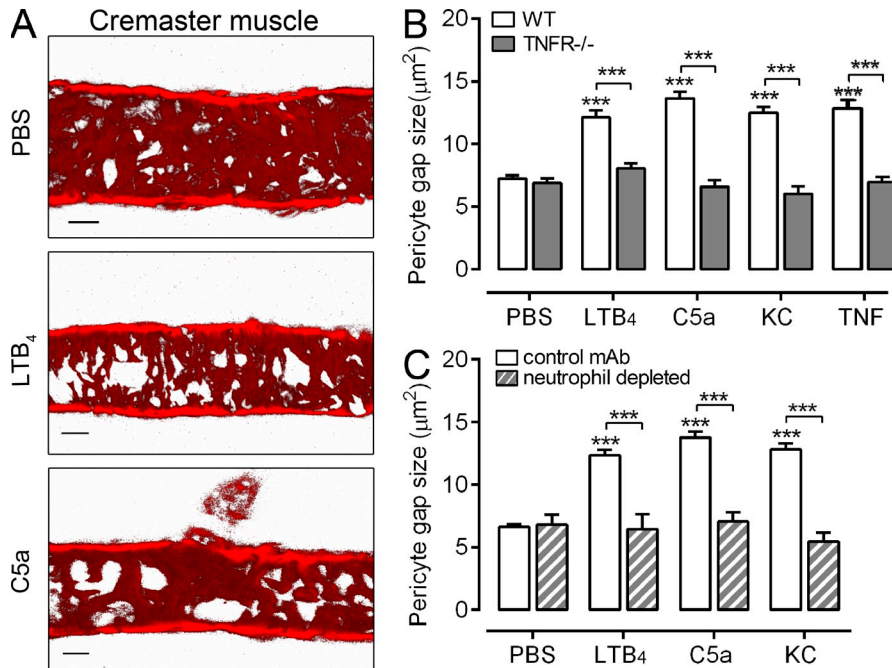
Figure 1. TNF mediates chemoattractant-induced changes in venular morphology. (A) Representative confocal images of post-capillary venules from five independently conducted control (PBS) or chemoattractant-stimulated cremaster muscles (4 h) labeled for pericytes (αSMA). Bar, 20 µm. (B) Pericyte gap size was quantified in cremasteric postcapillary venules of WT and TNFR$^{-/-}$ mice injected with PBS ($n = 10$ and 5, respectively), LTB$_4$ ($n = 12$ and 4, respectively), C5a ($n = 5$ and 4, respectively), KC ($n = 5$ and 4, respectively), or TNF ($n = 4$ and 3, respectively) for 2-4 h, involving 12 independent experiments. (C) As above but using control mice ($n = 3$ for PBS and LTB$_4$, $n = 5$ for C5a, $n = 6$ for KC) or mice depleted of their circulating neutrophils ($n = 3$ mice/group), involving 5 independent experiments. Six vessel segments per mouse were analyzed. Data are means ± SEM. Significant differences from PBS-treated tissues or other statistical comparisons (indicated by lines) are shown by asterisks. ***, P < 0.001.

before TEM, a response that was sustained during the breaching of the endothelium and remained elevated during neutrophil sub-EC crawling for observation periods of up to 45 min (Fig. 2, E and F). No such increase in signal was detected in mice injected with a control mAb. Collectively, these results provide direct evidence for the ability of LTB$_4$ to stimulate a rapid release of TNF from neutrophils in vitro and in vivo. In vivo, this response occurred when neutrophils were in close association with the venular wall, suggesting that neutrophil–EC interactions facilitate TNF release/cell surface expression and that endogenously generated TNF may regulate early neutrophil-dependent microvascular responses. These key issues were addressed in the studies detailed below.

Neutrophils in suspension, or adherent to ICAM–1 or ICAM–2, can rapidly release TNF in response to chemoattractants

Previous studies have indicated the importance of β_2 integrin-mediated neutrophil-EC adhesion in neutrophil–dependent increased microvascular permeability (Arfors et al., 1987; Gautam et al., 2000). To investigate the impact of this pathway on TNF release, purified neutrophils in suspension or adherent to ICAM-1 or ICAM-2 (key EC β_2 integrin ligands), were stimulated with LTB$_4$, C5a, or KC, and supernatants were assayed for TNF. LTB$_4$ was clearly able to stimulate TNF release from neutrophils in vitro and engagement of ICAM-1 or ICAM-2 was not a prerequisite for secretion under the conditions of these experiments, although there was a trend toward enhanced and/or accelerated TNF release from neutrophils adherent to ICAMs (Fig. 3 A). In contrast to LTB$_4$, the stimuli KC and C5a induced significant levels of TNF release from neutrophils only when the cells were adherent to ICAM-1 or ICAM-2 (Fig. 3 B). TNF secreted from stimulated

adherent neutrophils corresponded to ~43–88% of the total intracellular level of TNF. Collectively, these results demonstrate that EC β_2 integrin ligands can positively regulate TNF release from neutrophils although the extent of this priming effect is stimulus-specific.

Endogenous TNF mediates neutrophil–dependent increased microvascular permeability in vivo

As TNF expression was associated with neutrophil-venular wall interactions, we postulated that the release of this cytokine may change the barrier function of the EC monolayer. Locally administered neutrophil chemoattractants induced neutrophil infiltration into the cremaster muscle in WT mice, which were not significantly different in TNFR$^{-/-}$ mice (Fig. 4 A). These results indicate that endogenous TNF does not play a key role in mediating acute neutrophil infiltration induced by neutrophil chemoattractants in this model. However, vascular leakage induced by LTB$_4$ in the cremaster muscle, quantified as the local accumulation of i.v. injected Evans Blue, was abolished in TNFR$^{-/-}$ mice (Fig. 4 B). This phenomenon was also investigated in the mouse dorsal skin, where depletion of circulating neutrophils blocked microvascular leakage induced by LTB$_4$, but had no effect on the response to exogenous TNF (Fig. 4 C). In the dorsal skin, LTB$_4$, C5a, and KC were all found to induce rapid and transiently increased microvascular permeability, with the greatest plasma protein leakage being noted within the first 30 min after injection (Fig. 4 D). As observed using LTB$_4$ in the cremaster muscle, microvascular leakage induced by all of these stimuli was inhibited in the dorsal skin of TNFR$^{-/-}$ mice (Fig. 4 E), and chimeric mice generated by bone marrow transfer of TNF$^{-/-}$ hematopoietic stem cells into WT recipients (Fig. 4 F). The latter results specifically indicate the importance
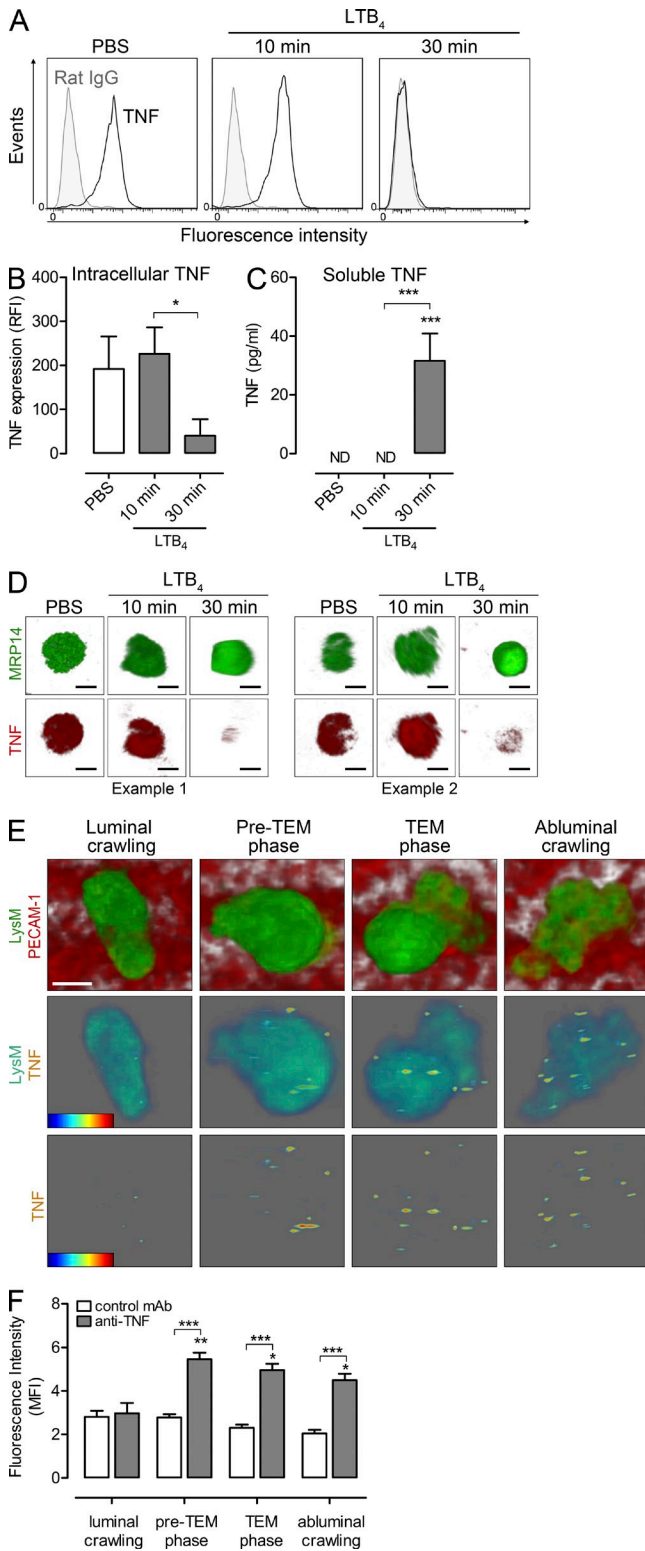
Figure 2. **Chemoattractants stimulate release of TNF from neutrophils in vitro and in vivo.** Mixed mouse blood leukocytes were treated with PBS (control) or stimulated with LTB$_4$ (10 or 30 min). Supernatants were assayed for soluble TNF by ELISA and cells were permeabilized and immunostained for analysis of intracellular TNF by flow cytometry and confocal microscopy. (A) Representative flow cytometry histograms from

of neutrophil–derived TNF in chemoattractant-induced microvascular leakage. Exogenous TNF was an effective inducer of increased microvascular permeability in the skin, a response that was undetectable in TNFR$^{-/-}$ mice, but as expected, was normal in the chimeric mice (Figs. 4, E and F). In line with our overall hypothesis that TNF mediates neutrophil-dependent increased microvascular permeability, exogenous TNF induced rapid plasma protein leakage. Specifically, the bulk of the response occurred within the first 30 min (Fig. 4 G) and significant vascular leakage was detected as early as 15 min after local administration of TNF (Fig. 4 H). A blocking anti–TNF mAb, when co-injected with LTB$_4$, also inhibited increased microvascular permeability, but this protocol had no impact on vascular leakage induced by the neutrophil–independent permeability-increasing mediator bradykinin (Fig. 4 I).

A model for neutrophil–dependent edema

In summary, we provide evidence for the involvement of endogenously generated TNF as a mediator of neutrophil-dependent increased microvascular permeability. Several permeability-increasing substances have been proposed as mediators of this process, including TNF (DiStasi and Ley, 2009), but direct evidence for a conclusive mechanism has been lacking. We propose the following sequence of events within the context of an acute inflammatory response. Chemoattractants generated in tissues in response to an inflammatory stimulus engage with their receptors on neutrophils within the venular lumen and trigger β_2-integrin activation. This induces rapid neutrophil adhesion, crawling on the venular wall, and the initiation of TEM mediated by the β_2 integrin EC ligands ICAM-1 and ICAM-2 (Phillipson et al., 2006; Ley et al., 2007; Woodfin et al., 2009; Halai et al., 2014). When

4 independent experiments showing the binding of anti-TNF mAb (black lines) or control IgG (filled). (B) Quantification of intracellular TNF by flow cytometry (expressed as RFI; $n = 6$ blood samples for PBS and 30 min LTB$_4$, $n = 5$ for 10 min LTB$_4$) from 4 independent experiments. (C) Quantification of released TNF ($n = 4$) from 4 independent experiments. ND, not detected. (D) Representative confocal images of neutrophils from two independent experiments show cells treated with PBS or LTB$_4$ (10 and 30 min) and stained for the neutrophil marker MRP-14 (green) or TNF (red). Bar, 5 µm. (E) Representative 3D-reconstructed images of LTB$_4$-stimulated cremasteric postcapillary venule (luminal side) showing GFP-neutrophils and PECAM-1–labeled ECs (red). The top panel shows neutrophils at different steps of the transmigration response, i.e., luminal crawling, preTEM phase (6 min before breaching ECs), TEM phase, and abluminal crawling. The associated TNF detected on the leukocyte surface for each step (intensity rainbow color code from blue [low intensity] to red [high intensity]) is shown in the bottom panels with and without the associated neutrophil. Bar, 5 µm. (F) Mean fluorescent intensity of signals on neutrophils was quantified in mice injected with anti-TNF or control mAbs ($n = 4$ mice/group) from 4 independent experiments. A total of ∼40 neutrophils were tracked and analyzed for each group. All data are means ± SEM. Statistical differences from PBS (B and C), signals from luminal crawling cells (F), or other comparisons (indicated by lines) are shown by asterisks. *, $P < 0.05$; **, $P < 0.01$; ***, $P < 0.001$.
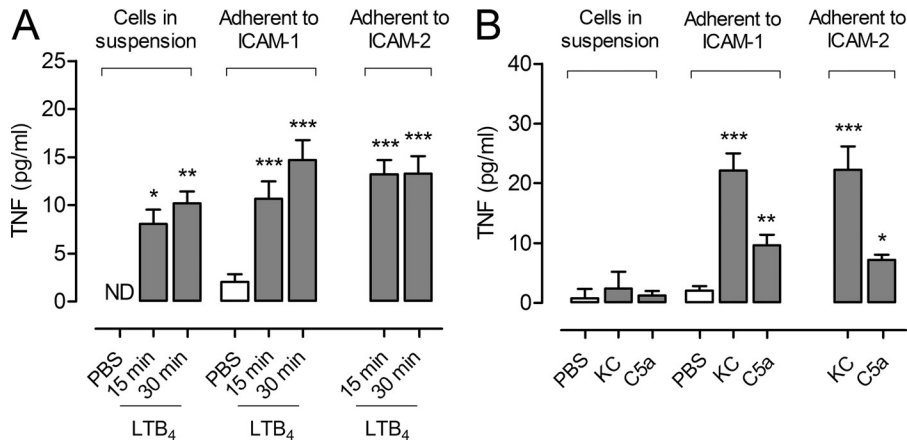
Figure 3. Neutrophils in suspension or adherent to ICAM-1 and ICAM-2 release TNF in response to chemoattractants. Purified neutrophils in suspension or after adhesion to ICAM-1– or ICAM-2–coated plates were stimulated with LTB_4 for 15 ($n = 5$, 7, and 7 samples, respectively) or 30 min ($n = 4$, 6, and 6 samples, respectively; A) or KC and C5a ($n = 3$) for 30 min (B). Control samples (in suspension or adherent to ICAM-1 o ICAM-2) were treated with PBS ($n = 6$, 7, and 7, respectively). Supernatants were assayed for TNF by ELISA. Graphs show means ± SEM of 3 independent experiments. ND, not detected. Significant differences from PBS control are indicated by asterisks. *, $P < 0.05$; **, $P < 0.01$; ***, $P < 0.001$.

the neutrophils are undergoing TEM or are located on the abluminal surface of ECs, chemoattractants induce the rapid surface expression and release of preformed TNF from the leukocytes, a response that can be up-regulated by adhesive interactions with ECs. The binding of TNF to its receptors on ECs stimulates the phosphorylation and endocytosis of the VE-cadherin complex in the junctions (Schulte et al., 2011) together with actomyosin contraction (Yuan, 2002), resulting in the opening of EC junctions and the leakage of plasma proteins. The signaling pathways that mediate TNF-induced increased EC permeability have been extensively studied and appear to involve activation of the small GTPase Rac (Cain et al., 2010) and the phosphatidylinositol (3,4,5)-trisphosphate–dependent Rac exchanger 1 (P-Rex1; Naikawadi et al., 2012).

As TNF is both secreted from neutrophils and is a neutrophil secretagogue, it is potentially possible that under some inflammatory conditions TNF may act cooperatively with other neutrophil-derived EC permeability factors. Of importance, we have found that neutrophil-dependent microvascular leakage is unaffected in neutrophil elastase$^{-/-}$ mice and in animals treated with ROS inhibitors (unpublished data). However, other factors may act synergistically with TNF, e.g., neutrophil-derived heparin-binding protein (HBP; CAP37, azurocidin), which has been implicated in neutrophil-dependent plasma leakage (Gautam et al., 2001; Di Gennaro et al., 2009). High concentrations of recombinant HBP have been shown to increase endothelial permeability, a charge-dependent effect (Gautam et al., 2001) similar to that of other very basic molecules such as polylysine (Needham et al., 1988). Supernatants from LTB_4-stimulated neutrophils have been reported to increase endothelial permeability, a response lost after incubation of supernatants with a solid phase polyclonal antibody to HBP (Di Gennaro et al., 2009). However, based on our observations, such supernatants would be expected to contain TNF, which may be removed by the antibody as a consequence of ionic interactions between highly positively charged HBP and the negatively charged cytokine. At lower concentrations, HBP is able to augment neutrophil adhesion (Lee et al., 2003) and may facilitate the retention

of anionic TNF on the venular endothelium, with both effects potentially contributing to a synergism between HBP and TNF.

As the perivascular BM is regarded as freely permeable to plasma proteins, the remodeling of the BM and the concomitant increases in gaps between adjacent pericytes that we observed (the starting point in this study) may have little effect on the rate of passage of plasma proteins into the tissues. Such changes in pericyte and BM morphology may be more relevant to the extravasation of blood-borne cells, microorganisms, or high molecular weight immune complexes under certain circumstances.

These observations provide an explanation for the rapid neutrophil-dependent microvascular plasma protein leakage induced by neutrophil chemoattractants in vivo (Wedmore and Williams, 1981) and its inhibition by an anti-β_2 integrin mAb (Arfors et al., 1987). As in the mouse, human neutrophils are also able to secrete TNF (Smedman et al., 2009). Thus, therapeutic TNF inhibitors may owe part of their efficacy in chronic inflammatory diseases to the mechanisms postulated here. Further, the use of TNF inhibitors might be considered, or revisited, for other conditions, particularly those where acute microvascular leakage is a life-threatening component.

MATERIALS AND METHODS

Mice. TNF receptors p55 and p75 double knockout mice (TNFR$^{-/-}$) on a C57BL/6 background were from The Jackson Laboratory and C57BL/6 WT mice from Harlan–Olac were used as controls. Lys-EGFP-ki mice (backcrossed to C57BL/6 for at least eight generations), exhibiting EGFP^{high} fluorescent neutrophils (Faust et al., 2000), were used with the permission of T. Graf (Albert Einstein College of Medicine, Bronx, NY) and were provided by M. Sperandio (Ludwig Maximilians University, Munich, Germany). Chimeric mice deficient in leukocyte TNF were generated by lethal irradiation of C57BL/6 WT mice (5.5 Gy twice, 4 h apart) and injection of bone marrow cells (1.5×10^6 cells/recipient i.v.) from TNF$^{-/-}$ mice (gift from V. Quesniaux, Centre National de la Recherche Scientifique Orleans, France). C57BL/6 WT littermates receiving WT bone marrow were used as controls. Mice were used between 6–12 wk of age. All animal experiments were conducted according to The Animals (Scientific Procedures) Act 1986 Amendment Regulations 2012 (SI 2012/3039), all projects are reviewed and approved by the Animal Welfare and Ethical Review Board (AWERB) within Queen Mary University of London.
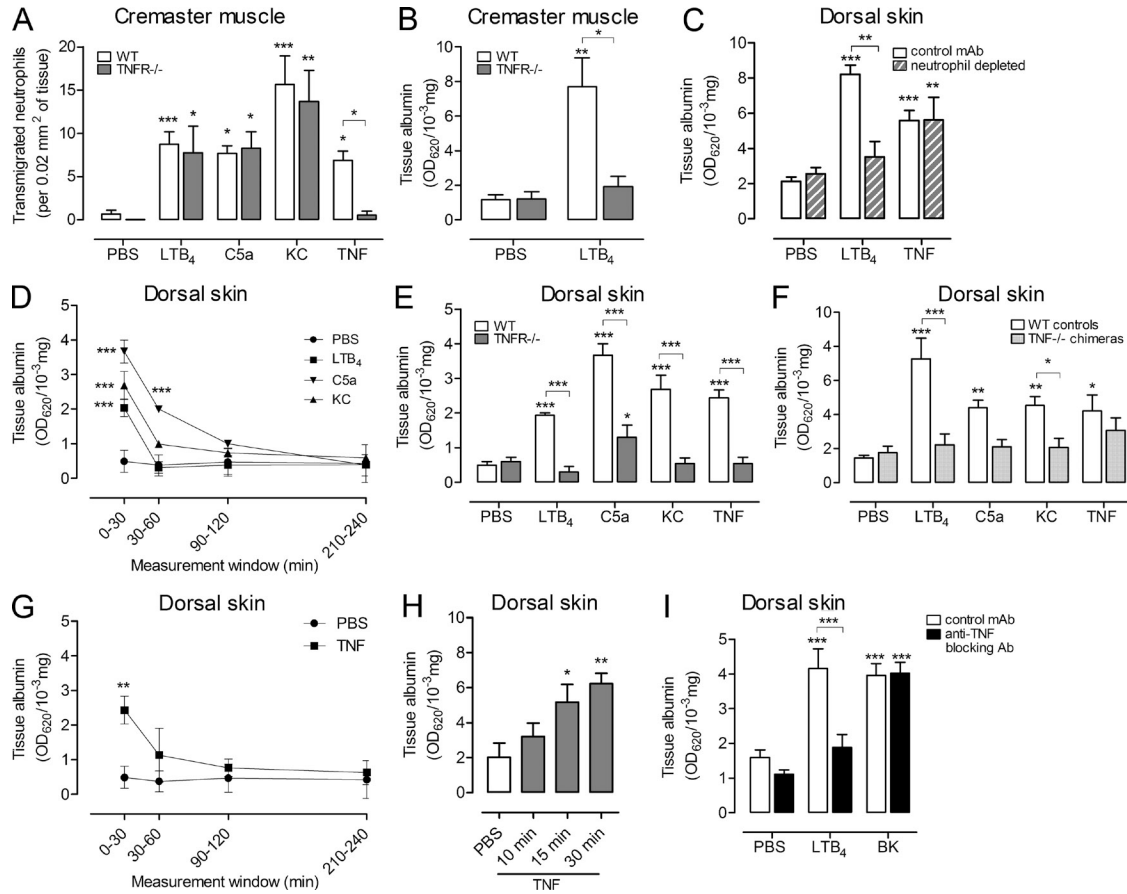
Figure 4. TNF mediates chemoattractant–induced microvascular leakage. (A) Neutrophil transmigration was quantified in cremasteric postcapillary venules of WT and TNFR$^{-/-}$ mice injected with PBS ($n = 11$ and 5 mice, respectively), LTB$_4$ ($n = 25$ and 4, respectively), C5a ($n = 8$ and 4, respectively), KC ($n = 5$ and 4, respectively), or TNF ($n = 4$ and 3, respectively) for 2-4 h involving 23 independent experiments. (B) Vascular leakage was analyzed in the cremaster muscle of WT and TNFR$^{-/-}$ mice treated with PBS ($n = 4$ and 3 mice, respectively) or LTB$_4$ (4 h; $n = 4$ and 3 mice, respectively) from 4 independent experiments. (C) Vascular leakage in the dorsal skin of WT or neutrophil-depleted mice after i.d. injection of PBS ($n = 9$ and 8 mice, respectively), LTB$_4$ ($n = 3$ mice), or TNF ($n = 6$ and 5 mice, respectively; 4h) from 3 independent experiments. (D) Kinetics of vascular leakage in the dorsal skin of WT mice injected i.d. with PBS ($n = 9$), LTB$_4$ ($n = 3$), C5a ($n = 3$), or KC ($n = 3$) from 3 independent experiments. (E) Vascular leakage in the dorsal skin of WT or TNFR$^{-/-}$ mice injected i.d. with PBS ($n = 9$ mice/group), or the indicated stimuli (30 min; $n = 3$ mice/group) from 3 independent experiments. (F) Vascular leakage in the dorsal skin of TNF$^{-/-}$ chimeric mice or control mice injected i.d. with PBS or the indicated stimuli (30 min; $n = 8$ mice/group) from 3 independent experiments. (G) Kinetics of vascular leakage in the dorsal skin of WT mice injected i.d. with PBS ($n = 9$) or TNF ($n = 3$) from 3 independent experiments. (H) Time course of vascular leakage in the dorsal skin of WT mice injected i.d. with PBS or TNF ($n = 4$ mice/group) from 3 independent experiments. (I) Vascular leakage in the dorsal skin of WT mice was analyzed after i.d. injection of PBS, LTB$_4$, or BK when co-injected with a control mAb ($n = 10$) or an anti-TNF blocking mAb ($n = 8$) using a 30 min reaction time from 3 independent experiments. All datasets are means ± SEM. Statistically significant differences from PBS treatment or other comparisons (indicated by lines) are shown by asterisks. *, $P < 0.05$; **, $P < 0.01$; ***, $P < 0.001$.

Induction of cremasteric inflammatory reactions and ex vivo analysis of tissues by confocal microscopy. Male mice were anaesthetized by i.m. injection of 1 ml/kg ketamine (40 mg)/xylazine (2 mg) in saline. LTB$_4$ (30 ng; Merck), C5a (300 ng; R&D Systems), KC (500 ng; AbD Serotec), or TNF (300 ng; R&D Systems) in 300 µl PBS or PBS alone were administered intrascrotally. Reaction times were as indicated, i.e., 2 h (KC and TNF) or 4 h (LTB$_4$, C5a, and IL-1β). At the end of each in vivo test period, mice were sacrificed and cremaster muscles were prepared for immunofluorescence staining and subsequent ex vivo analysis as previously described (Wang et al., 2006). In brief, cremaster muscles were fixed in 4% paraformaldehyde at 4°C, blocked and permeabilized in 10% normal goat serum, 10% FCS, and 0.5% Triton X-100 at room temperature. To visualize pericytes and neutrophils, tissues were incubated with primary antibodies anti–αSMA-Cy3 (1A4; Sigma-Aldrich) and anti–MRP-14 (gift from N. Hogg, Cancer Research UK, London, England) conjugated to Alexa Fluor 647. 3D confocal images were

captured using a LSM 5 PASCAL confocal laser-scanning microscope (Carl Zeiss) incorporating a 40× water-dipping objective (numerical aperture 0.8, resolution 0.37 µm). Z-stack images of half postcapillary venules (20–45 µm diam) were captured using the multiple track scanning mode at a resolution of 800 × 800 pixels in the x × y plane. The size (area) of gaps between adjacent pericytes and the number of transmigrated neutrophils were analyzed in postcapillary venules using ImageJ (National Institutes of Health) or IMARIS (Bitplane), respectively, as described previously (Wang et al., 2006; Voisin et al., 2010). In brief, 3D-reconstructed confocal images of half vessels (vessels were split along the longitudinal axis) were artificially displayed on a 2D surface (z-projection, maximum intensity) and converted into 8-bit grayscale projections. Gaps between adjacent pericytes (αSMA-negative regions) were either manually encircled across 200-µm vessel segments, or automatically quantified by ImageJ. The values of all ROI areas/vessel segment were cumulated and an average unit area of at least 4 vessel segments per mouse were quantified and plotted

as mean per mouse. Neutrophil transmigration was quantified by counting MRP-14^{+} cells around and within 50 µm from both sides of the vessel. At least 6 vessel segments per mouse were quantified and plotted as mean per mouse.

Neutrophil depletion. In some experiments, mice were depleted of their circulating neutrophils before tissue stimulation as previously described (Voisin et al., 2009). In brief, anti-GR1 antibody (25 µg/day; RB6-8C5; BD) in 500 µl saline was injected i.p. for 3 consecutive days. Control mice received rat IgG2bκ isotype control antibody (AbD Serotec). The level of neutrophils and monocytes was determined by flow cytometry (Gr1^{+} and Gr1^{+}/CX$_3$CR$_1$-GFP^{+} cells, respectively) from blood samples taken from the tail vein before and after antibody treatment. Mice treated with anti-Gr1 antibody showed >85% depletion of their circulating neutrophils with no impact on the proportion of blood Gr1^{+}/CX$_3$CR$_1$-GFP[+] monocytes.

Intravital confocal microscopy. Visualization of TNF release by neutrophils in vivo was analyzed by intravital confocal microscopy. Male Lys-EGFP-ki mice, anaesthetized by i.p. injection of ketamine (100 mg/kg) and xylazine (10 mg/kg), received an i.v. injection of a nonblocking dose of an anti-TNF mAb (4 µg, MP6-XT22; eBioscience) directly conjugated to Alexa Fluor 647, or rat IgG1κ isotype control antibody. Cremaster muscles were prepared for intravital imaging as previously described (Woodfin et al., 2011; Proebstl et al., 2012) and superfused with Tyrode's solution containing 10^{-8} M of LTB$_4$ for 2 h. Z-stack images of postcapillary venules were captured using an SP5 confocal microscope (Leica) incorporating a 20× water-dipping objective (NA 1.0) for 2 h. Images were acquired every minute for a total duration of 45 min with sequential scanning of different channels at a resolution of 1,024 × 512 pixels in the x × y plane and 0.7-µm steps in z-direction. Labeling of ECs was performed by intrascrotal injection of a nonblocking anti–PECAM-1 mAb conjugated with Alexa Fluor 555 (C390; eBioscience; 2 µg/mouse) at least 2 h before the exteriorization of the cremaster muscle. 4D confocal image sequences were then analyzed offline using IMARIS software, enabling the dynamic interaction of neutrophils with ECs to be observed, tracked, and analyzed in 3D. Specifically, ∼40 isolated cells from $n = 4$ animals for each group (i.e., i.v. injected anti-TNF or control Ab treated animals) were tracked during luminal crawling, transendothelial cell migration, and, finally, subendothelial cell (abluminal) motility within the vessel wall. An iso-surface volume was generated within the leukocyte channel (i.e., EGFP) for every time point of the indicated steps of the transmigration response. Mean fluorescent intensity (MFI) of the TNF/isotype control Ab channel within the leukocyte surface was quantified over time (i.e., within 45 min after LTB$_4$ stimulation) and normalized to the first step of transendothelial migration (i.e., formation of an EC junctional pore within the PECAM-1 channel). For clarity, the results of TNF MFI on the leukocyte are shown grouped for four different steps of the transmigration cascade, namely luminal crawling of neutrophils along the endothelium (∼15 min before breaching the EC layer), pretransendothelial cell migration (preTEM) phase (6 min before breaching the endothelium), TEM phase (duration of ∼6 min), and abluminal/subendothelial crawling (>20 min).

Permeability assay. Vascular leakage was assessed using the Mile's assay as previously described (Colom et al., 2012). In brief, mice were anaesthetized by i.p. injection of ketamine (100 mg/kg) and xylazine (10 mg/kg). Evans blue dye (0.5% in PBS, 5 µl/g) was injected i.v. and LTB$_4$ (30 ng), C5a (300 ng), KC (500 ng), TNF (300 ng), and bradykinin (100 µg; Sigma-Aldrich) in 50 µl PBS or PBS alone were administered intradermally into the back skin or intrascrotally and analyzed for the indicated in vivo test periods. In some experiments, tissues were co-injected with the stimulus of interest and an anti-TNF blocking antibody (100 µg, MP6-XT22; eBioscience) or an isotype-matched control mAb. To analyze the rate of vascular leakage over certain time windows (0–30, 30–60, 90–120, and 210–240 min of the inflammatory response), inflammatory stimuli were injected intradermally at different time-points (4, 2, 1, and 0.5 h) before the animals were sacrificed. Evans blue was injected for the last ∼28 min of the experiment. At the end of the experiment, animals were sacrificed, and sites of stimulation were harvested and incubated in formamide (Sigma-Aldrich)

at 56°C for 24 h. The amount of accumulated Evans blue in the tissue supernatant was quantified by spectroscopy at 620 nm.

Isolation and adhesion assay of blood neutrophils. Murine blood neutrophils were isolated using an anti–Ly-6G MicroBead kit (MACS; Miltenyi Biotec) according to the manufacturer's protocol (∼93% neutrophil purity was obtained as determined by flow cytometry). Cells, pooled from 4–6 mice (2 × 10^5 cells in 100 µl RPMI containing 10% FCS and 25 mM HEPES), were seeded onto 16-well Laboratory-Tek glass chamber slides (Thermo Fisher Scientific) precoated with rhICAM-1 (2.5 µg/ml) or rmICAM-2 (10 µg/ml; both from R&D Systems) and allowed to adhere for 30 min at 37°C before being stimulated with LTB$_4$ (10 nM), KC (3 nM), or C5a (3 nM). Control cells received PBS only. For comparison, purified neutrophils kept in suspension in LoBind tubes (Eppendorf) were also stimulated with chemoattractants or PBS. Supernatants were taken after 15 or 30 min stimulation and assayed for TNF by ELISA (eBioscience; sensitivity of 8 pg/ml). Total neutrophil intracellular content of TNF was quantified as ∼25 pg/ml as measured in cell lysates of samples containing 2 × 10^6 neutrophils/ml. Adhesion to slides was quantified by DAPI staining and IMARIS analysis.

Stimulation and analysis of blood leukocytes by flow cytometry and confocal microscopy. Whole blood was collected from WT mice and red blood cells were lysed with AKC lysis buffer (150 mM NH4Cl, 1 mM KHCO3, and 0.1 mM EDTA). Mixed blood leukocytes, pooled from 2–3 mice (2 × 10^6 cells in 1 ml) were stimulated with 10 nM LTB$_4$ in PBS complemented with 0.25% FCS, 1 mM CaCl, 1 mM MgCl, and 5 mM glucose for 10 or 30 min at 37°C. Supernatants were recovered for ELISA and stored at −80°C. Cells were washed twice at 500 g for 10 min at 4°C and analyzed by flow cytometry or confocal microscopy. For flow cytometry cells were co-stained for different leukocyte surface markers using the following antibodies: anti–Ly6G-PE (1A8; BioLegend; neutrophils), anti–CD115-A488 (AFS98; eBioscience; monocytes), anti–CD45-PE/Cy5 (RA3-6B2; BioLegend; pan-leukocyte marker), and anti–CD3e-PE-Cy5 (145-2C11; eBioscience; T cells). For intracellular cytokine detection and MRP-14 labeling (for confocal microscopy only), cells were fixed and permeabilized using BD Cytofix/Cytoperm Kit (BD), and stained with an anti-TNF Ab (MP6-XT22), or isotype-matched control Ab (conjugated to Alexa Fluor 647 or 555, respectively), or anti-MRP14 Ab conjugated to Alexa Fluor 488. For confocal microscopy cells were further stained with the nuclear dye DRAQ5. Surface and intracellular expression of molecules of interest were measured by flow cytometry on a FACSFortessa (BD) and analyzed using FlowJo software (Tree Star) (neutrophils were gated as Ly6G^{+} CD45^{+} CD115^{−} CD3^{−} cells) or a LSM 5 PASCAL confocal laser-scanning microscope (Carl Zeiss) incorporating a 63× oil-dipping objective (NA 1.4) analyzed with IMARIS.

Statistical analyses. Data are presented as means ± SEM of at least 3 independent experiments. Statistical differences between groups were analyzed using Student's t test or ANOVA followed by Dunnett or Bonferroni multiple comparison tests. P values <0.05 were considered significant.

REFERENCES

Arfors, K.E., C. Lundberg, L. Lindbom, K. Lundberg, P.G. Beatty, and J.M. Harlan. 1987. A monoclonal antibody to the membrane glycoprotein complex CD18 inhibits polymorphonuclear leukocyte accumulation and plasma leakage in vivo. *Blood*. 69:338–340.

Björk, J., P. Hedqvist, and K.E. Arfors. 1982. Increase in vascular permeability induced by leukotriene B4 and the role of polymorphonuclear leukocytes. *Inflammation*. 6:189–200. http://dx.doi.org/10.1007/BF00916243

Brett, J., H. Gerlach, P. Nawroth, S. Steinberg, G. Godman, and D. Stern. 1989. Tumor necrosis factor/cachectin increases permeability of endothelial cell monolayers by a mechanism involving regulatory G proteins. *J. Exp. Med.*169:1977–1991. http://dx.doi.org/10.1084/jem.169.6.1977

Cain, R.J., B. Vanhaesebroeck, and A.J. Ridley. 2010. The PI3K p110alpha isoform regulates endothelial adherens junctions via Pyk2 and Rac1. *J. Cell Biol.*188:863–876. http://dx.doi.org/10.1083/jcb.200907135

Colom, B., Y. Poitelon, W. Huang, A. Woodfin, S. Averill, U. Del Carro, D. Zambroni, S.D. Brain, M. Perretti, A. Ahluwalia, et al. 2012. Schwann cell-specific JAM-C-deficient mice reveal novel expression and functions for JAM-C in peripheral nerves. *FASEB J.*26:1064–1076. http://dx.doi.org/10.1096/fj.11-196220

Di Gennaro, A., E. Kenne, M. Wan, O. Soehnlein, L. Lindbom, and J.Z. Haeggström. 2009. Leukotriene B4-induced changes in vascular permeability are mediated by neutrophil release of heparin-binding protein (HBP/CAP37/azurocidin). *FASEB J.*23:1750–1757. http://dx.doi.org/10.1096/fj.08-121277

DiStasi, M.R., and K. Ley. 2009. Opening the flood-gates: how neutrophil-endothelial interactions regulate permeability. *Trends Immunol.*30:547–556. http://dx.doi.org/10.1016/j.it.2009.07.012

Faust, N., F. Varas, L.M. Kelly, S. Heck, and T. Graf. 2000. Insertion of enhanced green fluorescent protein into the lysozyme gene creates mice with green fluorescent granulocytes and macrophages. *Blood.* 96:719–726.

Gautam, N., H. Herwald, P. Hedqvist, and L. Lindbom. 2000. Signaling via beta(2) integrins triggers neutrophil-dependent alteration in endothelial barrier function. *J. Exp. Med.*191:1829–1839. http://dx.doi.org/10.1084/jem.191.11.1829

Gautam, N., A.M. Olofsson, H. Herwald, L.F. Iversen, E. Lundgren-Akerlund, P. Hedqvist, K.E. Arfors, H. Flodgaard, and L. Lindbom. 2001. Heparin-binding protein (HBP/CAP37): a missing link in neutrophil-evoked alteration of vascular permeability. *Nat. Med.*7:1123–1127. http://dx.doi.org/10.1038/nm1001-1123

Halai, K., J. Whiteford, B. Ma, S. Nourshargh, and A. Woodfin. 2014. ICAM-2 facilitates luminal interactions between neutrophils and endothelial cells in vivo. *J. Cell Sci.*127:620–629. http://dx.doi.org/10.1242/jcs.137463

Huber, A.R., and S.J. Weiss. 1989. Disruption of the subendothelial basement membrane during neutrophil diapedesis in an in vitro construct of a blood vessel wall. *J. Clin. Invest.*83:1122–1136. http://dx.doi.org/10.1172/JCI113992

Hurley, J.V. 1964. Acute inflammation: The effect of concurrent leukocytic emigration and increased permeability on particle retention by the vascular wall. *Br. J. Exp. Pathol.*45:627–633.

Lee, T.D., M.L. Gonzalez, P. Kumar, P. Grammas, and H.A. Pereira. 2003. CAP37, a neutrophil-derived inflammatory mediator, augments leukocyte adhesion to endothelial monolayers. *Microvasc. Res.*66:38–48. http://dx.doi.org/10.1016/S0026-2862(03)00010-4

Ley, K., C. Laudanna, M.I. Cybulsky, and S. Nourshargh. 2007. Getting to the site of inflammation: the leukocyte adhesion cascade updated. *Nat. Rev. Immunol.*7:678–689. http://dx.doi.org/10.1038/nri2156

Majno, G., and G.E. Palade. 1961. Studies on inflammation. 1. The effect of histamine and serotonin on vascular permeability: an electron microscopic study. *J. Biophys. Biochem. Cytol.*11:571–605. http://dx.doi.org/10.1083/jcb.11.3.571

Naikawadi, R.P., N. Cheng, S.M. Vogel, F. Qian, D. Wu, A.B. Malik, and R.D. Ye. 2012. A critical role for phosphatidylinositol (3,4,5)-trisphosphate-dependent Rac exchanger 1 in endothelial junction disruption and vascular hyperpermeability. *Circ. Res.*111:1517–1527. http://dx.doi.org/10.1161/CIRCRESAHA.112.273078

Needham, L., P.G. Hellewell, T.J. Williams, and J.L. Gordon. 1988. Endothelial functional responses and increased vascular permeability induced by polycations. *Lab. Invest.*59:538–548.

Phillipson, M., B. Heit, P. Colarusso, L. Liu, C.M. Ballantyne, and P. Kubes. 2006. Intraluminal crawling of neutrophils to emigration sites: a molecularly distinct process from adhesion in the recruitment cascade. *J. Exp. Med.*203:2569–2575. http://dx.doi.org/10.1084/jem.20060925

Proebstl, D., M.B. Voisin, A. Woodfin, J. Whiteford, F. D'Acquisto, G.E. Jones, D. Rowe, and S. Nourshargh. 2012. Pericytes support neutrophil subendothelial cell crawling and breaching of venular walls in vivo. *J. Exp. Med.*209:1219–1234. http://dx.doi.org/10.1084/jem.20111622

Schulte, D., V. Küppers, N. Dartsch, A. Broermann, H. Li, A. Zarbock, O. Kamenyeva, F. Kiefer, A. Khandoga, S. Massberg, and D. Vestweber. 2011. Stabilizing the VE-cadherin-catenin complex blocks leukocyte extravasation and vascular permeability. *EMBO J.*30:4157–4170. http://dx.doi.org/10.1038/emboj.2011.304

Smedman, C., B. Gårdlund, K. Nihlmark, P. Gille-Johnson, J. Andersson, and S. Paulie. 2009. ELISpot analysis of LPS-stimulated leukocytes: human granulocytes selectively secrete IL-8, MIP-1beta and TNF-alpha. *J. Immunol. Methods.* 346:1–8. http://dx.doi.org/10.1016/j.jim.2009.04.001

Tokita, K., and T. Yamamoto. 2004. Differential role of neutrophils and monocytes during subcutaneous plasma extravasation. *Lab. Invest.*84:1174–1184. http://dx.doi.org/10.1038/labinvest.3700133

Voisin, M.B., A. Woodfin, and S. Nourshargh. 2009. Monocytes and neutrophils exhibit both distinct and common mechanisms in penetrating the vascular basement membrane in vivo. *Arterioscler. Thromb. Vasc. Biol.*29:1193–1199. http://dx.doi.org/10.1161/ATVBAHA.109.187450

Voisin, M.B., D. Pröbstl, and S. Nourshargh. 2010. Venular basement membranes ubiquitously express matrix protein low-expression regions: characterization in multiple tissues and remodeling during inflammation. *Am. J. Pathol.*176:482–495. http://dx.doi.org/10.2353/ajpath.2010.090510

Wang, S., M.B. Voisin, K.Y. Larbi, J. Dangerfield, C. Scheiermann, M. Tran, P.H. Maxwell, L. Sorokin, and S. Nourshargh. 2006. Venular basement membranes contain specific matrix protein low expression regions that act as exit points for emigrating neutrophils. *J. Exp. Med.*203:1519–1532. http://dx.doi.org/10.1084/jem.20051210

Wedmore, C.V., and T.J. Williams. 1981. Control of vascular permeability by polymorphonuclear leukocytes in inflammation. *Nature.* 289:646–650. http://dx.doi.org/10.1038/289646a0

Williams, T.J., and P.J. Jose. 1981. Mediation of increased vascular permeability after complement activation. Histamine-independent action of rabbit C5a. *J. Exp. Med.*153:136–153. http://dx.doi.org/10.1084/jem.153.1.136

Williamson, L.M., K. Sheppard, J.M. Davies, and J. Fletcher. 1986. Neutrophils are involved in the increased vascular permeability produced by activated complement in man. *Br. J. Haematol.*64:375–384. http://dx.doi.org/10.1111/j.1365-2141.1986.tb04131.x

Woodfin, A., M.B. Voisin, B.A. Imhof, E. Dejana, B. Engelhardt, and S. Nourshargh. 2009. Endothelial cell activation leads to neutrophil transmigration as supported by the sequential roles of ICAM-2, JAM-A, and PECAM-1. *Blood.*113:6246–6257. http://dx.doi.org/10.1182/blood-2008-11-188375

Woodfin, A., M.B. Voisin, M. Beyrau, B. Colom, D. Caille, F.M. Diapouli, G.B. Nash, T. Chavakis, S.M. Albelda, G.E. Rainger, et al. 2011. The junctional adhesion molecule JAM-C regulates polarized transendothelial migration of neutrophils in vivo. *Nat. Immunol.*12:761–769. http://dx.doi.org/10.1038/ni.2062

Yancey, K.B., L. Bielory, R. Wright, N. Young, M.M. Frank, and T.J. Lawley. 1987. Patients with bone marrow failure demonstrate decreased cutaneous reactivity to human C5a. *J. Invest. Dermatol.*88:388–392. http://dx.doi.org/10.1111/1523-1747.ep12469445

Yuan, S.Y. 2002. Protein kinase signaling in the modulation of microvascular permeability. *Vascul. Pharmacol.*39:213–223. http://dx.doi.org/10.1016/S1537-1891(03)00010-7